



## Research article

# Embelin attenuates lipopolysaccharide-induced acute kidney injury through the inhibition of M1 macrophage activation and NF- $\kappa$ B signaling in mice

Qiao Tang<sup>a,b</sup>, Yun Tang<sup>b,c</sup>, Qun Yang<sup>d</sup>, Rong Chen<sup>b</sup>, Hong Zhang<sup>b,e</sup>, Haojun Luo<sup>b</sup>, Qiong Xiao<sup>b</sup>, Kaixiang Liu<sup>b</sup>, Liming Huang<sup>b</sup>, Jie Chen<sup>f</sup>, Lin Wang<sup>g</sup>, Xinrou Song<sup>b</sup>, Sipei Chen<sup>b</sup>, Guisen Li<sup>b,c</sup>, Li Wang<sup>b,c</sup>, Yi Li<sup>b,c,\*</sup>

<sup>a</sup> North Sichuan Medical College, Nanchong, 637000, Sichuan, China

<sup>b</sup> Department of Nephrology, Sichuan Provincial People's Hospital, Sichuan Clinical Research Center for Kidney Diseases, University of Electronic Science and Technology of China, Chengdu, 610072, Sichuan, China

<sup>c</sup> Chinese Academy of Sciences Sichuan Translational Medicine Research Hospital, Chengdu, 610072, Sichuan, China

<sup>d</sup> Department of Pathology, School of Medicine, Sichuan Academy of Medical Science and Sichuan Provincial People's Hospital, University of Electronic Science and Technology of China, Chengdu, 610072, Sichuan, China

<sup>e</sup> Southwest Medical University, Luzhou, 646000, Sichuan, China

<sup>f</sup> Central Laboratory, Sichuan Academy of Medical Science and Sichuan Provincial People's Hospital, University of Electronic Science and Technology of China, Chengdu, 610072, Sichuan, China

<sup>g</sup> Institute of Laboratory Animal Sciences, School of Medicine, Sichuan Academy of Medical Science and Sichuan Provincial People's Hospital, University of Electronic Science and Technology of China, Chengdu, 610072, Sichuan, China

## ARTICLE INFO

## Keywords:

Embelin  
Septic acute kidney injury  
Inflammation  
Macrophage  
Phosphorylated NF- $\kappa$ B p65 translocation

## ABSTRACT

Septic acute kidney injury (AKI) is commonly associated with renal dysfunction and high mortality in patients. Owing to the rapid and violent occurrence of septic AKI with inflammation, there are no effective therapies to clinically treat it. Embelin, a natural product, has a potential regulatory role in immunocytes. However, the role and mechanism of embelin in septic AKI remains unknown. This study aimed to elucidate the role of embelin in macrophage regulation in lipopolysaccharide (LPS)-induced septic AKI. Embelin was intraperitoneally administered to mice after LPS injection. And bone marrow-derived macrophages (BMDMs) were subsequently isolated from the mice to explore the immunomodulatory role of embelin in macrophages. We found that embelin attenuated renal dysfunction and pathological renal damage in the LPS-induced sepsis mouse model. Molecular docking predicted that embelin could bind to phosphorylated NF- $\kappa$ B p65 at the ser536 site. Embelin inhibited the translocation of NF- $\kappa$ B p65 via phosphorylation at ser536 in LPS-induced AKI. It also reduced the secretion of IL-1 $\beta$  and IL-6 and increased the secretion of IL-10 and Arg-1 of BMDMs and mice after LPS stimulation, indicating that embelin suppressed macrophage M1 activation in LPS-induced AKI. Therefore, embelin attenuated LPS-induced septic

**Abbreviations:** AKI, acute kidney injury; LPS, lipopolysaccharide; BMDMs, bone marrow-derived macrophages; BUN, blood urea nitrogen; Scr, serum creatinine; DMEM, Dulbecco's modified eagle's medium; FBS, fetal bovine serum; HE, hematoxylin & eosin; ICU, intensive care unit; PAS, periodic-acid Schiff; IHC, immunohistochemistry; mIF, multiplex immunofluorescent.

\* Corresponding author. Department of Nephrology, Sichuan Provincial People's Hospital, Sichuan Clinical Research Center for Kidney Diseases, University of Electronic Science and Technology of China, Chengdu, 610072, Sichuan, China.

E-mail address: [liyisn@med.uestc.edu.cn](mailto:liyisn@med.uestc.edu.cn) (Y. Li).

<https://doi.org/10.1016/j.heliyon.2023.e14006>

Received 26 July 2022; Received in revised form 27 January 2023; Accepted 17 February 2023

Available online 26 February 2023

2405-8440/© 2023 The Authors. Published by Elsevier Ltd. This is an open access article under the CC BY-NC-ND license (<http://creativecommons.org/licenses/by-nc-nd/4.0/>).

AKI by suppressing NF- $\kappa$ B p65 at ser536 in activated macrophages. This study preclinically suggests a therapeutic role of embelin in septic AKI.

## 1. Introduction

Sepsis is defined as life-threatening organ dysfunction caused by a dysregulated host response to infection [1]. Acute kidney injury (AKI) is a frequent complication of septic patients in intensive care units, and about 50% of all septic patients are likely to develop sepsis-related AKI accompanied by a marked increase in mortality [2,3]. According to the Sepsis 3.0 guidelines, severe AKI patients are often given multiple interventions, such as antibiotics, diuretics, fluid therapy, and avoiding the use of nephrotoxic drugs [1]. Owing to the rapid and violent occurrence of septic AKI, which is associated with many complex inflammatory signals and cytokines, there are no effective therapies or medications to clinically treat it [4]. Therefore, it is particularly urgent to find novel effective targets and therapeutic molecules for septic AKI.

Natural products are one of the main sources of medications and important lead compounds for the treatment of major human diseases. Some compounds derived from natural products have been preclinically reported to alleviate AKI by regulating renal disorders [5,6]. Salidroside could protect rats against septic AKI by inhibiting inflammation and apoptosis [7], isoliquiritigenin attenuates septic acute kidney injury by regulating ferritinophagy-mediated ferroptosis [8], and curcumin could protect against AKI by regulating the release of immunomodulators and oxygen free radicals, and reducing apoptosis and mitochondrial dysfunction [9–11]. Although a wide range of natural products show clinical treatment potential for septic AKI, most of them are still in the preclinical research stage owing to problems with low solubility, low bioavailability, and inappropriate dosage. Therefore, it is urgent to find effective and

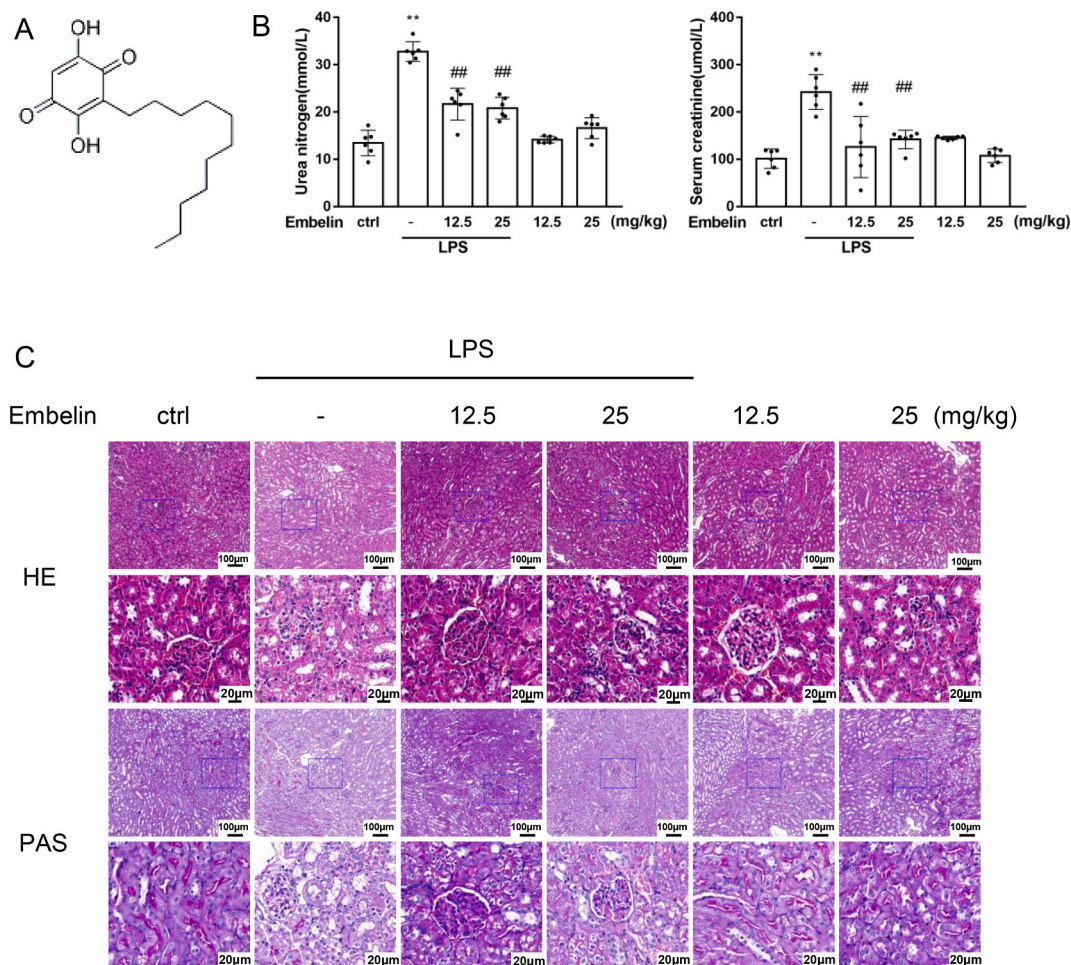


**Fig. 1.** Embelin protects the kidney from LPS induced AKI. A) Embelin chemical formula. B) The levels of BUN and Scr in mice after LPS injection *in vivo* (n = 6 per group). \*\*p < 0.01 compared with the control group; ##p < 0.01 compared with the LPS group. C) H&E and PAS staining of renal tissues from C57BL/6 mice treated with or without LPS and/or embelin for 24 h. The images represent three independent experiments, and data are presented as mean  $\pm$  standard deviation (SD). The scale bars shown are 20  $\mu$ m or 100  $\mu$ m.

appropriate natural products for the treatment of septic AKI.

Embelin, a benzoquinone-derivative isolated from *Embelia ribes*, has potential antibacterial, antidiabetic, antioxidant, analgesic, antifertility, and anti-cancer activity [12–15]. Embelin could block NF- $\kappa$ B signaling to suppress NF- $\kappa$ B regulated antiapoptotic and metastatic gene products [16], and it possesses a potential immunocyte regulatory role in acute liver injury and allergic asthma [17, 18]. However, the role and mechanism of embelin in septic AKI remains unknown.

This study was performed to demonstrate the effect and action mechanism of embelin on septic AKI. Thus, a murine septic AKI model and a bone marrow-derived macrophage (BMDM) cell model were established, both induced by lipopolysaccharides (LPS). To assess the effect of embelin in septic AKI induced by LPS, we investigated the renal function, pathological changes in the kidney, serum level of inflammatory cytokines, activation of macrophages, and immunomodulatory signaling. This study demonstrates the potentially protective role of embelin against septic AKI in mice, via immunocyte regulation and immunomodulatory signal pathway.

## 2. Materials and methods

### 2.1. Compounds and reagents

Embelin was obtained from Selleck Company (S7025, Selleck Chemicals, Houston, TX, USA); its chemical formula is shown in Fig. 1A. The NF- $\kappa$ B activator betulinic acid (BA, S3603) and dexamethasone phosphate disodium (DEX, S5956) were also purchased from Selleck Company. *Escherichia coli* serotype O111:B4 lipopolysaccharides were purchased from Sigma-Aldrich (L2630, Sigma, USA). Isoliquiritigenin (ISL) was purchased from MedChemExpress (HY-N0102, Princeton, USA). The kit for nuclear and cytoplasmic extraction was purchased from Thermo Fisher Scientific (8833, Waltham, MA, USA).

### 2.2. Animal studies

All experiments involving mice were performed according to the Ethics Committee of the Sichuan Provincial People's Hospital (2020-215), and obtained approval after review by the Instructional Animal Care and Use Committee (IACUC). Male Balb/C mice, aged 4–6 weeks and weighing 14–16 g, were used for the isolation of BMDMs. Male wild-type C57BL/6 mice, aged 6–8 weeks and weighing 18–22 g were randomly allocated to the following eight groups (n = 6 per group): the control, LPS, 12.5 mg/kg embelin, 25 mg/kg embelin, 12.5 mg/kg embelin plus LPS, 25 mg/kg embelin plus LPS, DEX plus LPS, and ISL plus LPS groups. All mice were obtained from Dossy Experimental Animals Co. Ltd (Chengdu, China) and housed at the Animal Center of Scientific Study at Sichuan Provincial People's Hospital. All mice in this study drank and ate freely throughout the day and night cycles. Mice were intraperitoneally injected with LPS at a dose of 10 mg/kg to induce septic AKI. Then, 12.5 or 25 mg/kg embelin was administered to the mice 1 h post LPS injection. For the DEX plus LPS group, 5 mg/kg DEX was administered to the mice. For the ISL plus LPS group, the mice were treated with 50 mg/kg ISL. Mice in the control group and LPS group received equal volumes (200  $\mu$ L) of the vehicle containing 5% dimethyl sulfoxide, 5% Tween 80, 40% PEG300, and 50% ddH<sub>2</sub>O. Twenty-four hours after LPS injection, the mice were anesthetized and then sacrificed to collect blood and renal tissue samples for further study.

### 2.3. Cell culture and pretreatment

The human renal tubular epithelial cell line HK2 was purchased from the Chinese Academy of Sciences (Wuhan, China) and identified by Short Tandem Repeat (STR). The cells were cultured in Dulbecco's modified eagle's medium F12 (DMEM-F12, Gibco, Waltham, MA, USA) containing 10% gibco fetal bovine serum, 100 mg/mL streptomycin, and 100 U/mL penicillin (Hyclone, Logan, UT, USA) in a 5% CO<sub>2</sub> atmosphere at 37 °C. Cell passages of 7–14 were used in the experiments.

Balb/c mice were sacrificed after an intraperitoneal injection of 50 mg/kg pentobarbital. Then, the femur was isolated and cells were extracted from the bone marrow. The isolated BMDMs were cultured in DMEM with 20% fetal bovine serum. For macrophage differentiation, BMDMs were stimulated with GM-CSF (10 ng/mL, MEOPP-07021, Cyagen, Santa Clara, CA, USA) for 7 days [19]. Then, the BMDMs were collected for identification using flow cytometry. For the embelin treatment, the BMDMs cells were treated with 1 or 5  $\mu$ M of embelin for 24 h. Additionally, BMDMs were treated with 1  $\mu$ g/mL LPS or 4  $\mu$ M of the NF- $\kappa$ B activator BA for 24 h. The BMDMs were then collected using cell scrapers for further study.

### 2.4. ELISA assessment

We used enzyme-linked immunosorbent assay (ELISA) to detect the cytokine levels of serum or cell supernatants [20]. For murine serum detection, mice were pretreated with 12.5 or 25 mg/kg embelin, followed by a 10 mg/kg LPS injection. BMDM supernatants were generated by culturing  $1 \times 10^4$  cells/well in 96 well plates with embelin, BA, and LPS treatment. Following the manufacturer's instructions, 50  $\mu$ L of the samples and standards were added to the corresponding wells. Then, horseradish peroxidase (HRP)-conjugated antibody was added, and the samples were incubated for 60 min at 37 °C. After washing and allowing the chromogenic reaction to occur, the absorbance at OD 450 was measured using a microplate reader (#680, Bio-Rad, USA). ELISA kits for IL-1 $\beta$  (#ZC37974), IL-6 (#ZC37988), Arg-1 (#ZC38342), and IL-10 (#ZC37962) were provided by the Zcibio Technology Company (Shanghai, China).

## 2.5. Cytotoxicity assay

HK2 cells were seeded in 96 well plates at a density of  $1 \times 10^4$  cells/well. After incubation overnight, HK2 cells were incubated with 0, 1.25, 2.5, 5, 10, 20, 40, and 80  $\mu$ M embelin for 24 h. Cytotoxicity in the HK2 cells was detected using cell counting kit-8 assay (CCK-8, CK04, Dojindo, Japan). According to the manufacturer's instructions, 10  $\mu$ L of the CCK-8 reagent was added to each well, and 6 wells were included in each concentration. The absorbance was measured at 450 nm wavelength using a microplate reader (#680, Bio-Rad) after 3 h incubation. The concentration-dependent curve of embelin-treated HK2 cells was generated using the following formula: cell viability = (A450 of test - A450 of blank)/(A450 of control - A450 of blank)  $\times$  100%. Then, the 50% inhibitory concentration (IC<sub>50</sub>) was calculated in GraphPad prism software (version 7) using the cell viability and the logarithm of the embelin concentration.

## 2.6. Histopathology and immunohistochemistry

After fixing with formalin and embedding in paraffin, murine renal tissues were cut into 2  $\mu$ m sections. The murine renal tissue sections were analyzed using hematoxylin and eosin (H&E) staining and periodic acid-Schiff (PAS) staining. Six randomly selected fields of view were chosen to score necrosis according to the following criteria: "0" indicated normal renal tubules, "1" indicated <10% necrotic renal tubules, "2" indicated 11–25% necrotic renal tubules, "3" indicated 26–75% necrotic renal tubules, and "4" indicated >75% necrotic renal tubules [21,22]. The primary antibodies used for immunohistochemical staining were the CD68 (1:200, ab955, Abcam, Cambridge, UK), CD206 (1:200, 87887, Cell Signaling Technology, Danvers, MA, USA), iNOS (1:100, ab115819, Abcam), and CD163 (1:500, ab182422, Abcam) antibodies.

## 2.7. Multiplex immunofluorescence and confocal microscopy

After deparaffinization and rehydration, renal tissue sections underwent antigen retrieval, blocking and antibody incubation. The primary antibodies included anti-KIM-1 (1:100, #NBP2-43761, Novus, USA), CD206 (1:200, #87887, Cell Signaling Technology), and iNOS (1:100, ab115819, Abcam). After incubation with the three antibodies, the nuclei were stained with DAPI for 5 min at 25 °C. Each section was observed using an Opal 4-color IHC kit (#NEL821001KT, Akoya Biosciences, MA, USA) containing Opal 520, Opal 570, Opal 690, and spectral DAPI. The multiplex TSA immunostaining tissue sections were observed under a confocal microscope (#LSM900, ZEISS microscopy, Germany) equipped with a digital camera.

## 2.8. Bioinformatics analysis

Target prediction was performed to identify the potential targets of the drug or disease. The compound SMILES were retrieved from the PubChem database (<https://pubchem.ncbi.nlm.nih.gov/>), and embelin targets were identified using Swiss Target Prediction (<http://www.swisstargetprediction.ch/>). The AKI disease targets were obtained from the TTD and DisGeNET databases. The intersection of the two sets of targets was used to create a Venn diagram. The KOBAS database was employed to enrich the signal pathway.

## 2.9. Flow cytometry

The cells that were positive for CD68 expression could be recognized as macrophages [23,24]. To confirm that the BMDMs were successfully isolated, we performed flow cytometry to detect CD68. BMDMs were collected, washed twice in cold stain buffer, then stained with Viability Stain 510 (#564406, BD Biosciences, Franklin Lakes, NJ, USA) and APC anti-mouse CD68 antibody (#137007, BioLegend, CA, USA) for 30 min. The cells were then washed with pre-cold stain buffer and resuspended in 1% paraformaldehyde for flow cytometry analysis using a flow cytometer (#FACS Canto II, BD Biosciences). Next, the obtained data were analyzed using FlowJo software (Tree Star, Ashland, OR, USA).

## 2.10. Western blotting

Murine BMDMs and kidney tissues were lysed using RIPA buffer (#P0013B, Beyotime, China) containing phenylmethanesulfonyl fluoride (PMSF, #ST506-2, Beyotime). Proteins were separated using sodium dodecyl sulfate polyacrylamide gel electrophoresis (SDS-PAGE). The proteins were transferred from the gel to 0.45  $\mu$ m polyvinylidene fluoride (PVDF) membranes (#88518, Thermo Fisher Scientific). The membranes were blocked with 5% albumin bovine (#A8020, Solarbio, China) at 37 °C for 60 min and then incubated with the following primary antibodies at 4 °C overnight: phosphorylated NF- $\kappa$ B p65 (Ser536, 1:1000, #310013, Zen Bioscience, China), NF- $\kappa$ B p65 (1:1000, #380172, Zen Bioscience), Toll-Like Receptor 4 (TLR4; 1:1000, #505258, Zen Bioscience), phosphorylated I $\kappa$ B $\alpha$  (1:10000, #ab133462, Abcam), I $\kappa$ B $\alpha$  (1:1000, #380682, Zen Bioscience), and  $\beta$ -actin (1:5000, #380624, Zen Bioscience). Next, they were incubated with HRP-conjugated secondary antibodies from goats against mice (1:5000, #511103, Zen Bioscience) or rabbits (1:5000, #511203, Zen Bioscience). The enhanced chemiluminescence reagent (#1701102, Millipore, USA) was used to perform the coloration reaction on the membranes. The chemiluminescence signal was observed using an imaging system (Fusion FX7, Vilber Lourmat, France). The density of the bands was quantified using ImageJ software (64-bit Java 1.6.0). The total protein and cytoplasmic protein levels were normalized to those of the beta-actin antibody (8F10) (1:10000, 700068, HRP-conjugated mouse, Zen Bioscience), while the levels of nuclear proteins were normalized to those of PCNA (1:1000, #2009472E1, Zen Bioscience).

**Table 1**  
Weight and damage score in the animal model.

Group	Weight (g)	Damage score
Control	21.05 ± 0.68	0.33 ± 0.52
LPS	18.6 ± 0.18**	2.83 ± 0.41**
LPS + embelin 12.5	19.5 ± 0.37##	1.00 ± 0.63##
LPS + embelin 25	19.28 ± 0.42	0.83 ± 0.75##
Embelin 12.5	20.35 ± 0.15	0.33 ± 0.52
Embelin 25	20.58 ± 0.29	0.17 ± 0.41

Six fields of view were randomly selected from PAS stained samples to score. Data are expressed as means ± standard deviation (SD). \*\*p < 0.01 compared with the control group. ##p < 0.01 compared with the LPS group.

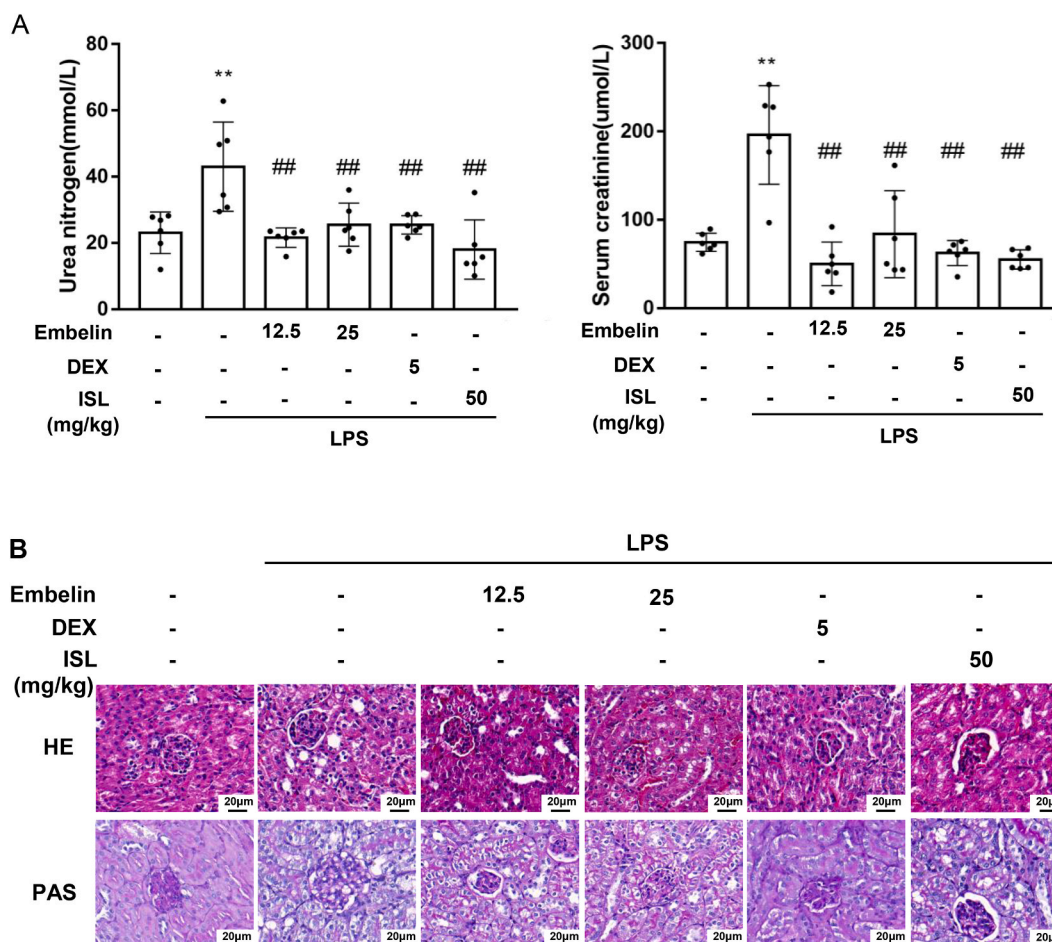


**Fig. 2.** Embelin, DEX, and ISL can alleviate LPS induced AKI in mice. A) The levels of BUN and Scr in LPS-treated mice (n = 6 per group). \*\*p < 0.01 compared with the control group; ##p < 0.01 compared with the LPS group. B) H&E and PAS staining of renal tissues from mice treated with LPS and/or embelin/DEX/ISL for 24 h. Images shown represent three independent experiments, and data are presented as mean ± standard deviation (SD). The scale bars shown are 20 μm.

### 2.11. Molecular docking

The small molecule structure of embelin was downloaded from the Pubchem database and transformed into a pdb format. It was then uploaded to the Autodocktool program to assign atomic types and add atomic charges, for molecular docking ligands. The 3D model of the receptor protein was constructed using the I-tasser online server according to NF-κB (Q04206). Default values were adopted for all parameters, and the model with the highest score was selected as the final protein model for molecular docking. AutoDock Vina 1.1.2 software was used for molecular docking. The ligand was set to be flexible and the receptor rigid. The search accuracy was set to 100 and default settings were used for the other parameters. The reasonable conformation was selected as the

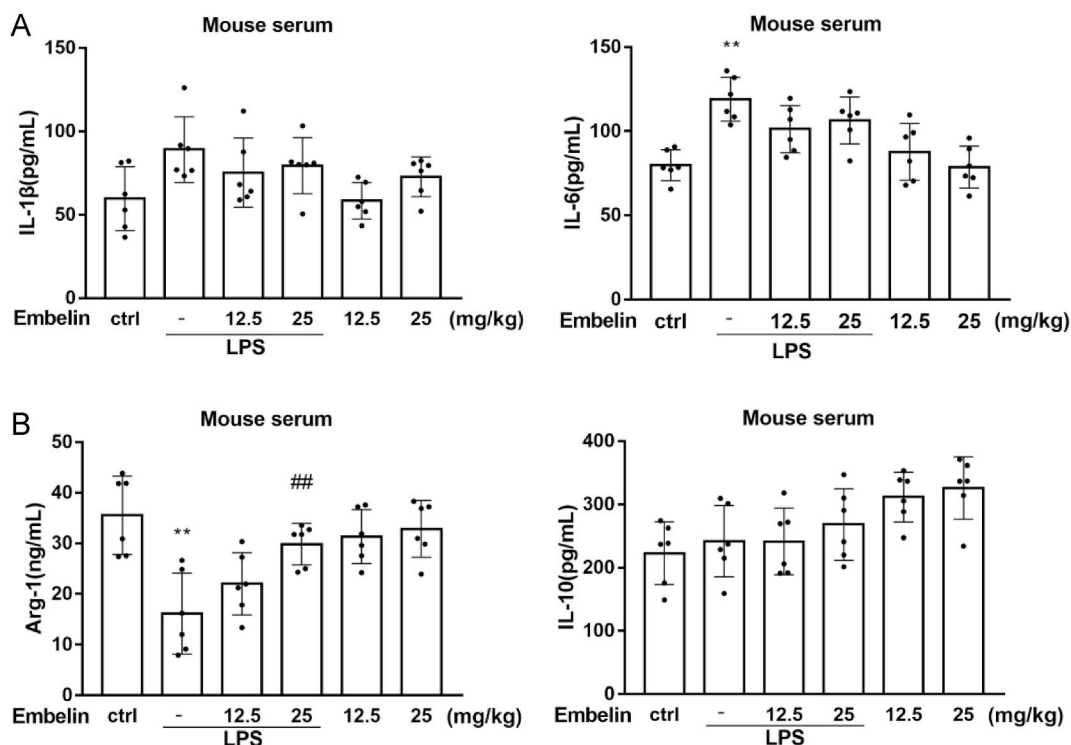


**Fig. 3.** Embelin inhibits the secretion of IL-1 $\beta$  and IL-6 and promotes the production of Arg-1 and IL-10 following LPS stimulation in mice. Mouse serum was collected to detect the levels of pro-inflammatory (IL-1 $\beta$  and IL-6) and anti-inflammatory (Arg-1 and IL-10) cytokines using ELISA. A) Detection of the serum levels of IL-1 $\beta$  and IL-6 in each group of mice. B) Assessment of the serum levels of Arg-1 and IL-10 in each group of mice. \*\* $p < 0.01$  compared with the control group; ##  $p < 0.01$  compared with the LPS group ( $n = 6$  per group). Images shown represent three independent experiments, and data are presented as mean  $\pm$  standard deviation (SD).

docking conformation for further analysis.

### 2.12. Statistical analysis

The data were checked for a normal distribution in GraphPad Prism version 7 and are expressed as mean  $\pm$  standard deviation. Two-tailed and unpaired  $t$ -tests were performed to evaluate the differences between two groups. One-way analysis of variance was used for multiple comparisons.  $P < 0.05$  was considered statistically significant.

## 3. Results

### 3.1. Embelin ameliorates renal injury after LPS injection

To examine the effect of embelin on AKI pathogenesis, we measured the levels of blood urea nitrogen (BUN) and serum creatinine (Scr), which are indicators of renal function. We determined that LPS injection could significantly increase the levels of BUN and Scr in mice, whereas embelin decreased the levels of BUN and Scr in LPS-treated mice (Fig. 1B). We also found severe renal tubular epithelial cell degeneration and swelling, and inflammatory cell infiltration in murine kidneys after LPS injection, and embelin substantially alleviated such pathological damage in the kidney (Fig. 1C). PAS staining revealed a reduction in the damage scores after embelin treatment in LPS-treated mice (Table 1). These findings indicate that embelin ameliorates renal injury in mice after LPS injection.

### 3.2. Embelin could alleviate acute renal injury after LPS injection equivalently to DEX and ISL

To identify the efficacy of embelin in septic AKI, we chose the clinical drug DEX and the new candidate natural drug ISL as positive controls. We found that BUN and Scr were significantly increased in the LPS group, and embelin (12.5 and 25 mg/kg), DEX, and ISL treatment could all reduce these levels in LPS-treated mice (Fig. 2A). Through routine renal histopathological detection using HE and PAS staining, we observed significant injury of the renal tubular epithelial cells, including degradation, vacuole formation, and nuclei disorganization, accompanied by tubular dilatation and the reduction or disappearance of the brush border in mice in the LPS group. However, embelin, DEX, and ISL treatment could all significantly attenuate these typical renal tubular cell injuries in LPS-injection-

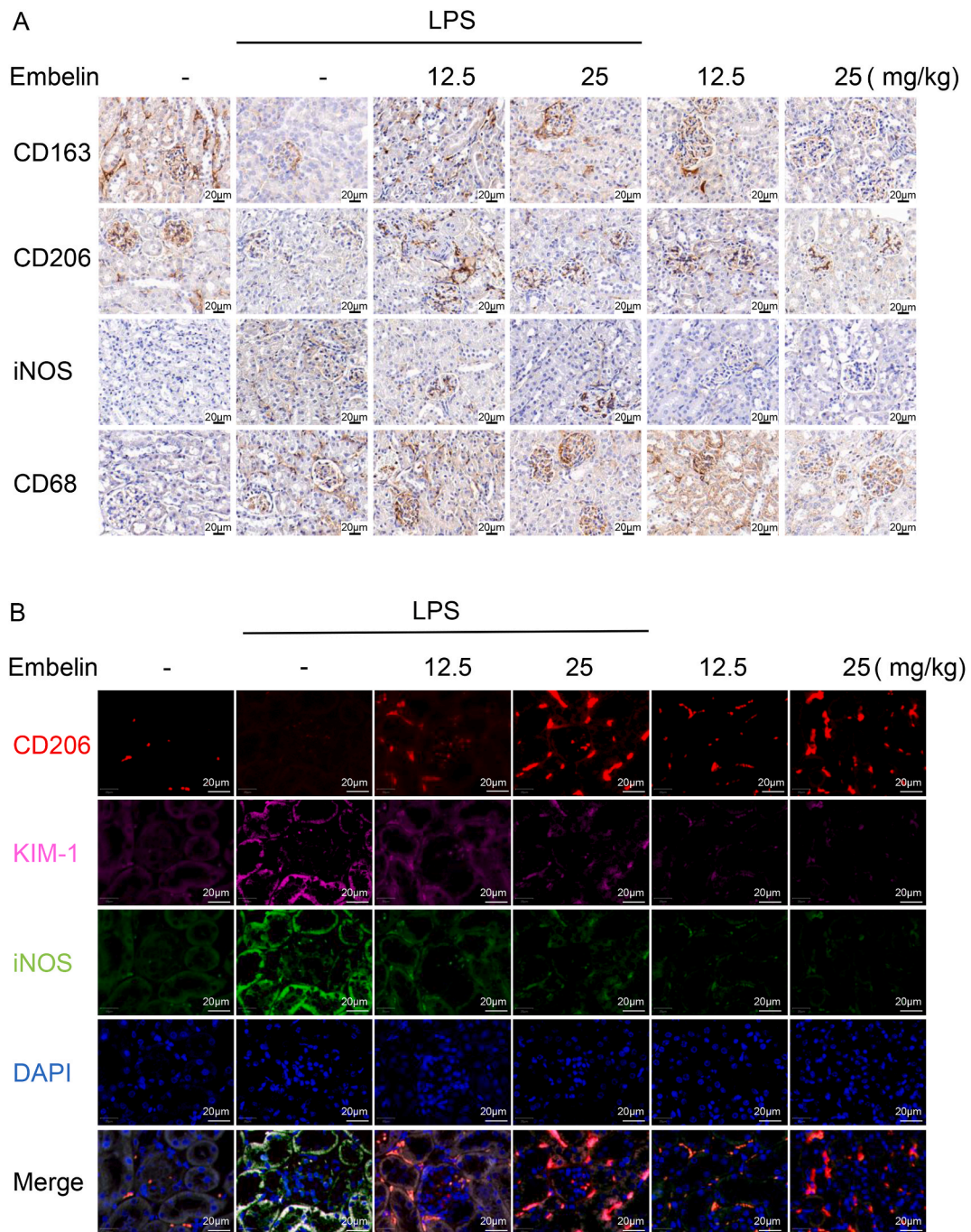


**Fig. 4.** Embelin inhibits the activation of M1 macrophages in the LPS mouse model. A) M1 marker (iNOS) and M2 markers (CD163 and CD206) were detected using IHC. B) KIM-1 (purple), CD206 (red), iNOS (green), and DAPI (blue) are illustrated through multiplex immunofluorescence. All fields were captured using confocal microscope using a 60 × oil immersion lens. The images shown are representative of three independent experiments. The scale bars shown are 20 μm. (For interpretation of the references to color in this figure legend, the reader is referred to the Web version of this article.)

induced septic AKI (Fig. 2B).

### 3.3. Embelin inhibits the levels of IL-1β and IL-6 and increases the secretion of Arg-1 and IL-10 in murine serum following LPS injection

To examine the effects of embelin on LPS-induced murine AKI, we measured the levels of inflammatory cytokines, such as IL-1β, IL-

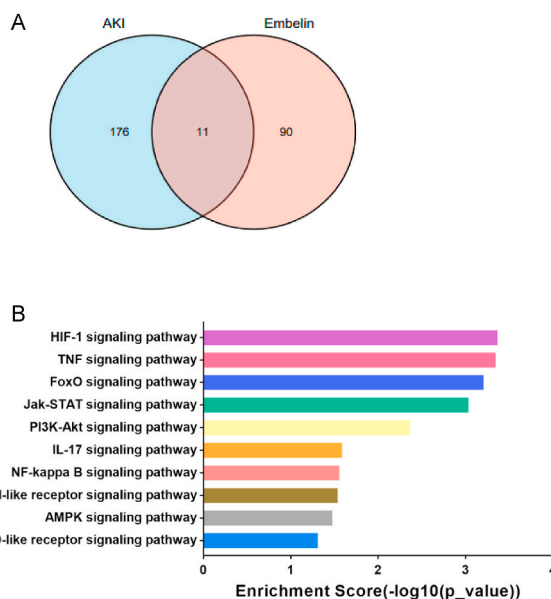


**Fig. 5. Bioinformatics analysis.** A) Venn diagram displaying overlapping genes associated with AKI and embelin. B) KEGG pathway enrichment analysis of overlapping targets indicated that the NF- $\kappa$ B signal pathway plays an important role in the embelin treatment of septic AKI.

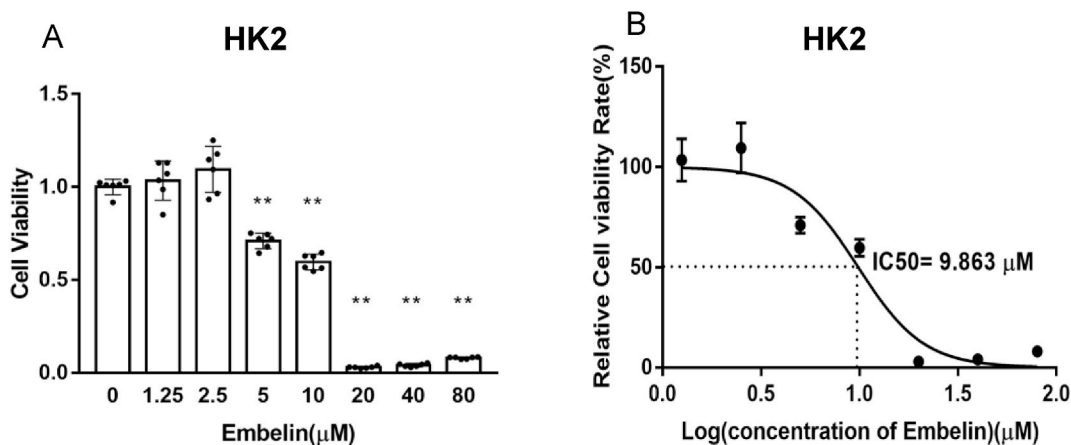


**Fig. 6. Embelin does not inhibit HK2 cell viability in a dose-dependent manner *in vitro*.** A) Cytotoxic effects of embelin on HK2 cells were assessed using the CCK-8 cell viability assay. \*\* $p < 0.01$  compared with the control group. B) IC<sub>50</sub> values of embelin against HK2 cells were obtained. Images shown represent three independent experiments, and data are presented as the mean  $\pm$  standard deviation (SD).

6, Arg-1, and IL-10 in mice treated with embelin after LPS injection. We observed an increase in the secretion of IL-1 $\beta$  and IL-6 in murine serum from the LPS group, whereas both the 12.5 and 25 mg/kg embelin treatments reduced the serum levels of IL-1 $\beta$  and IL-6 in LPS-treated mice (Fig. 3A). LPS reduced the secretion of serum Arg-1 and IL-10 in mice, whereas neither the 12.5 nor the 25 mg/kg embelin treatment decreased the levels of Arg-1 and IL-10 in LPS-injected mice. On the contrary, the 25 mg/kg embelin treatment significantly increased the Arg-1 levels in the serum of LPS-treated mice compared to that of LPS-treated mice that did not receive embelin treatment (Fig. 3B).

#### 3.4. Embelin inhibits M1 macrophage activation in LPS-induced AKI

Immunohistochemical staining of murine kidneys revealed that LPS increased the expression of CD68 and iNOS, whereas embelin treatment decreased the expression of iNOS. LPS also reduced the expression of CD163 and CD206, whereas embelin treatment recovered their expression in the renal tissues of LPS-treated mice (Fig. 4A). Immunofluorescence staining of CD206, KIM-1, and iNOS in murine renal tissues demonstrated that the LPS injection increased the expression of KIM-1 and iNOS and reduced the expression of CD206, whereas embelin treatment reduced the expression of KIM-1 and iNOS and increased the expression of CD206 in the renal



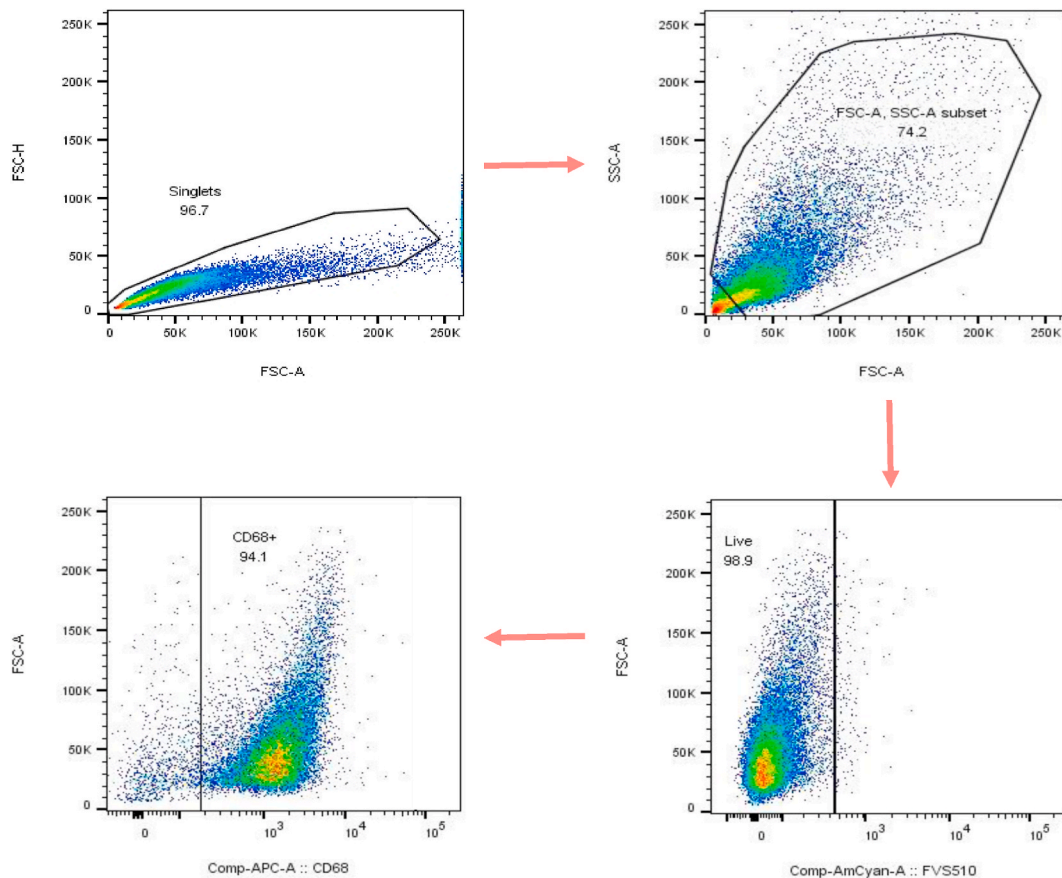


**Fig. 7. The identification of mature macrophages.** Prepared BMDMs were detected using flow cytometry with Viability Stain 510 and CD68. The images shown are representative of three independent experiments.

tissues of LPS-treated mice (Fig. 4B).

### 3.5. Bioinformatics analysis shows predicted targets and functional enrichment of embelin in AKI

To elucidate the therapeutic mechanisms of embelin in AKI, we performed bioinformatics analysis of embelin and AKI. After a systematic search of public databases, we obtained a total of 288 predicted target genes for both embelin and AKI. Of these, 187 were associated with AKI and 101 were associated with embelin, while 11 were associated with both AKI and embelin (Fig. 5A). We performed a Kyoto Encyclopedia of Genes and Genomes pathway enrichment analysis of the genes involved in both AKI and embelin. We observed notable inflammatory pathways associated with both AKI and embelin, including the NF- $\kappa$ B, TNF, Jak-STAT, and Toll-like receptor signaling pathways (Fig. 5B).

### 3.6. Embelin does not reduce the viability of HK2 cells

To assess the possible cytotoxic effects of embelin on renal tissues, we measured the viability of HK2 cells treated with embelin. A clear decline in the viability of HK2 cells after treatment with 1.25 and 2.5  $\mu$ M embelin was not observed. However, 5 and 10  $\mu$ M embelin decreased the viability of HK2 cells, and HK2 cell viability decreased significantly in the 20, 40, and 80  $\mu$ M embelin treatments (Fig. 6A). Analysis of the relative cell viability of HK2 cells revealed that the IC<sub>50</sub> of embelin in HK2 cells was 9.863  $\mu$ M (Fig. 6B).

### 3.7. Purity of mature macrophages

To identify the purity of mature BMDMs, we used CD68 for flow cytometry. The flow cytometry analysis results of Viability Stain 510 and CD68 revealed that 98.9% of the cells were viable and 94.1% of the cells were CD68-positive, indicating the successful isolation of murine BMDMs (Fig. 7).

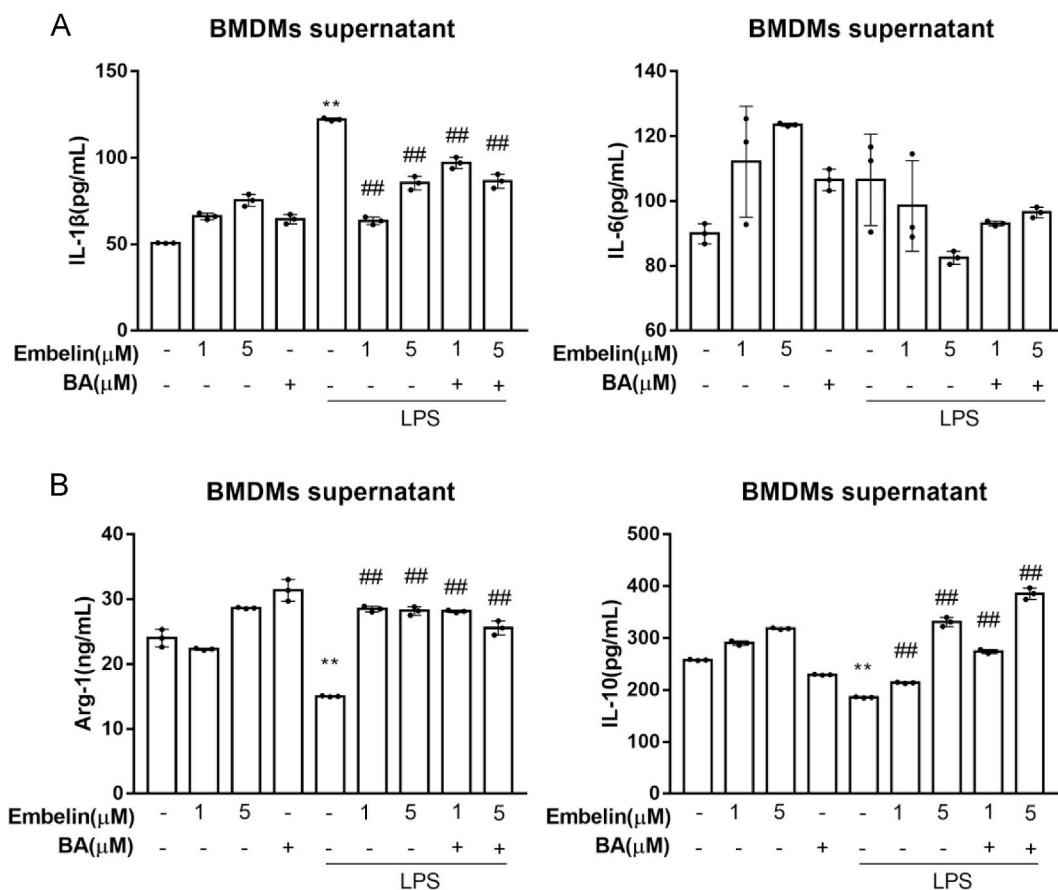


**Fig. 8.** Embelin inhibits IL-1 $\beta$  and IL-6 cytokines induced by LPS *in vitro*. The BMDMs were treated with GM-CSF (10 ng/mL) for seven days and then treated with or without varying concentrations of embelin in the presence or absence of BA and/or LPS for 24 h. The cell supernatant was collected and analyzed for IL-1 $\beta$ , IL-6, Arg-1, and IL-10 using ELISA. A) Levels of pro-inflammatory cytokines (IL-1 $\beta$  and IL-6) in each group were analyzed using ELISA. B) Levels of anti-inflammatory cytokines (Arg-1 and IL-10) in each group were analyzed using ELISA. \*\* $p < 0.01$  compared with the control group; ### $p < 0.01$  compared with the LPS group. Images shown are representative of three independent experiments, and data are presented as the mean  $\pm$  standard deviation (SD).

### 3.8. Embelin inhibits the levels of IL-1 $\beta$ and IL-6 and increases the levels of Arg-1 and IL-10 in BMDMs

LPS increased the levels of IL-1 $\beta$  and IL-6, but reduced the levels of Arg-1 and IL-10 in the supernatants of murine BMDMs. Conversely, embelin inhibited the secretion of IL-1 $\beta$  and IL-6, but increased the secretion of Arg-1 and IL-10 in the supernatants of both LPS-treated and BA-treated murine BMDMs (Fig. 8A and B).

### 3.9. Embelin inhibits the expression of NF- $\kappa$ B signaling *in vivo* and *in vitro*

Western blotting of murine renal tissues showed that LPS significantly increased the expression of TLR4 and the phosphorylation of I $\kappa$ B $\alpha$  and NF- $\kappa$ B p65, whereas both 12.5 and 25 mg/kg embelin reduced the expression of TLR4 and the phosphorylation of I $\kappa$ B $\alpha$  and NF- $\kappa$ B p65 in renal tissues of mice following LPS injection (Fig. 9A). Similarly, LPS stimulation increased the expression of TLR4 and the phosphorylation of I $\kappa$ B $\alpha$  and NF- $\kappa$ B p65 in murine BMDMs, whereas 1 and 5  $\mu$ M embelin inhibited the expression of TLR4 and the phosphorylation of I $\kappa$ B $\alpha$  and NF- $\kappa$ B p65 in murine BMDMs following LPS stimulation (Fig. 9B).

### 3.10. Molecular docking shows that embelin can bind to phosphorylated NF- $\kappa$ B p65 at the ser536 site

Docking studies that predict interactions between compounds and their target proteins is also crucial in drug research [25]. To test whether embelin could act on the ser536 site of phosphorylated NF- $\kappa$ B p65, we performed molecular docking simulation analysis. The 3D structure of embelin and phosphorylated NF- $\kappa$ B p65 are shown in Fig. 10 A and B. We found that embelin binds to a groove on the surface of the receptor protein and the two have good shape complementarity, with an affinity of 15.1 kJ/mol (Fig. 10C). The bonding groove had specific hydrophilicity and hydrophobicity (Fig. 10D). Embelin can form a hydrophilic interaction with the ser536 residue

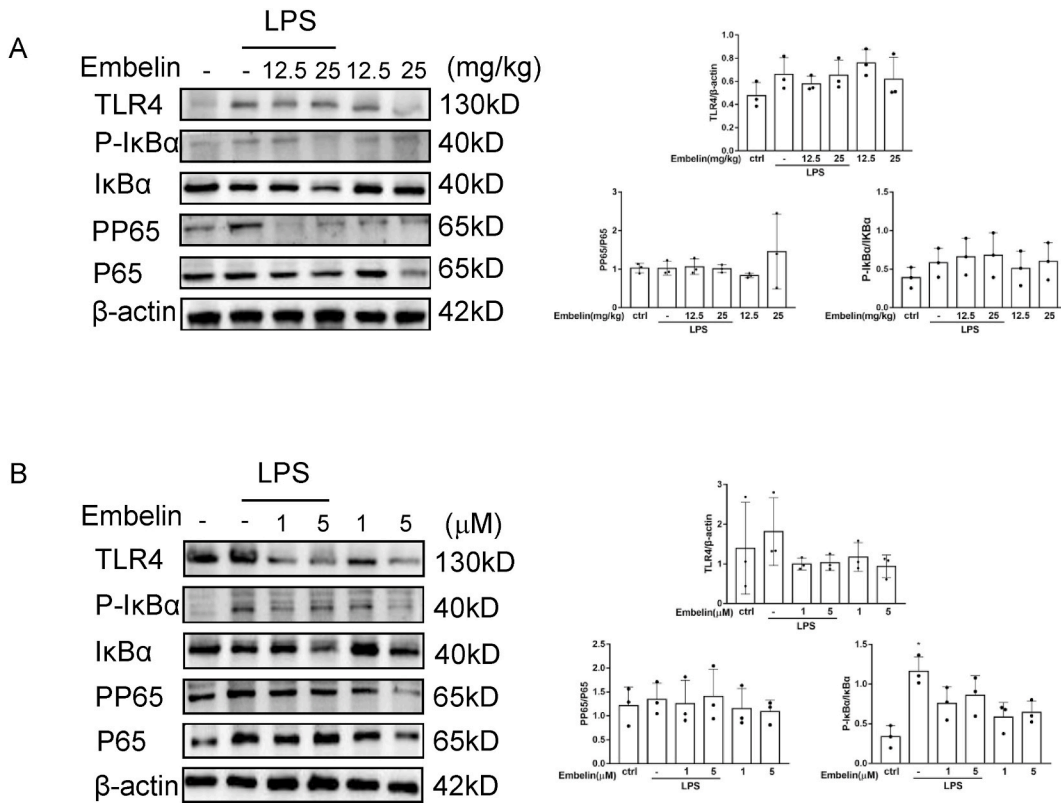


**Fig. 9. Embelin inhibits the NF-κB signaling pathway in septic AKI both *in vivo* and *in vitro*.** A) Total protein was extracted from the kidney tissues of mice injected with LPS and/or embelin at different concentrations and was analyzed using western blotting (WB). B) Total protein from mature murine BMDMs treated with or without embelin was extracted for WB. All bands were quantitatively analyzed with ImageJ software and are shown on the right. \*p < 0.05 compared with the control group. Images shown are representative of three independent experiments, and data are presented as the mean ± standard deviation (SD).

(phosphorylation), and the hydroxyl group of the embelin ligand can also form a hydrogen bond with the phosphorylation group of ser536 (Fig. 10E). In conclusion, embelin could act through the ser536 site of phosphorylated NF-κB p65.

**3.11. Embelin inhibits the expression of phosphorylated NF-κB p65 at ser536 of the nucleus *in vivo* and *in vitro***

Western blot results showed that LPS significantly increased the phosphorylation of NF-κB p65 at ser536 in the nucleus of murine renal tissues and BMDMs, whereas embelin significantly inhibited the phosphorylation of NF-κB p65 at ser536 in the nucleus of both murine renal tissues and BMDMs upon LPS stimulation. Similarly, embelin reduced NF-κB p65 levels in the cytoplasm of murine renal tissues and BMDMs (Fig. 11A and B).

**4. Discussion**

In this study, we determined that embelin treatment following LPS injection ameliorated renal injury. To further identify the efficacy of embelin in septic AKI, we chose the clinical drug DEX and the new candidate natural drug ISL as positive controls; embelin could suppress acute renal injury after LPS injection equivalently to DEX and ISL. These results indicate the protective role of embelin against septic AKI in murine kidneys. However, the mechanism by which embelin exerts its inhibitory effects on LPS-induced murine AKI remains unknown. As reported by previous studies, embelin has an immunomodulatory role against inflammation [26,27]. Macrophages play a pivotal role in infection, immune response to acute injury, and tissue repair during inflammation [28]. AKI is often triggered by an acute inflammatory response, causing renal injury [29,30]. In septic AKI, renal tubular epithelial cells become damaged and express KIM-1 [31]. Macrophages are also activated in septic AKI and may increase the expression of iNOS [32]. In elucidating the effects of embelin on macrophages in LPS-induced AKI, we observed that embelin treatment increased the expression of CD163 and CD206 in the kidney tissues of mice treated with LPS. Immunofluorescent staining of CD206, KIM-1, and iNOS in murine renal tissues showed that embelin administration inhibited the expression of KIM-1 and iNOS in murine kidneys following LPS injection. Moreover, embelin also increased the expression of CD206 in the kidneys of mice, suggesting its regulation of macrophage activation.

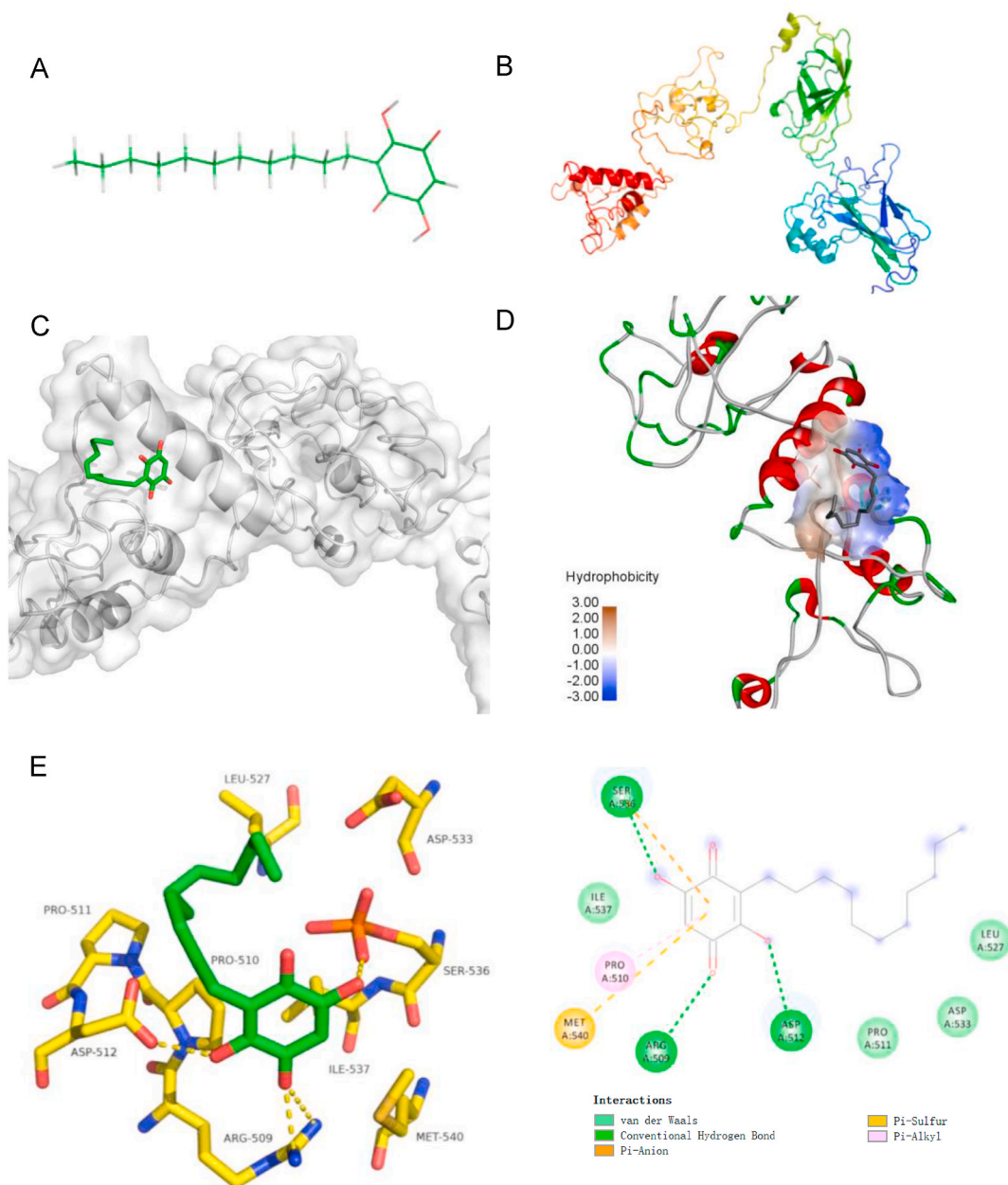


**Fig. 10. Molecular docking simulation analysis.** A) The 3D structure of ligand embelin. B) The 3D structure of receptor phosphorylated NF- $\kappa$ B p65. C) Embelin binds to a groove on the surface of the receptor protein. D) The bonding groove has specific hydrophilicity and hydrophobicity. E) Embelin can form a hydrophilic interaction with the ser536 residue (phosphorylation) and can also form a hydrogen bond with the phosphorylated group of ser536.

Macrophages can be classified based on their activation state. Classically activated pro-inflammatory M1 subtypes and repairing M2 subtypes exist [33,34]. M1 macrophages induce classical activation via LPS stimulation [35,36]. IL-1 $\beta$  and IL-6 are secreted by macrophages during M1 activation [37,38]. In our study, embelin treatment reduced the serum levels of IL-1 $\beta$  and IL-6 in LPS-treated mice. Furthermore, embelin inhibited the secretion of IL-1 $\beta$  and IL-6 and increased the secretion of Arg-1 and IL-10 in LPS-treated murine BMDMs. LPS increased the expression of IL-1 $\beta$  and IL-6 and reduced the secretion of Arg-1 and IL-10 in LPS-treated murine BMDMs. These findings suggest that embelin suppressed LPS-induced M1 macrophage polarization in mice and BMDMs.

Embelin at concentrations ranging from 5 to 80  $\mu$ M could inhibit the viability of HK2 cells. Analysis of the relative cell viability of HK2 cells showed that the IC<sub>50</sub> of embelin in HK2 cells was 9.863  $\mu$ M. In cell-free testing, the IC<sub>50</sub> of embelin was reported to be 4.1  $\mu$ M [39]. Therefore, we used 1 and 5  $\mu$ M embelin to treat murine BMDMs.

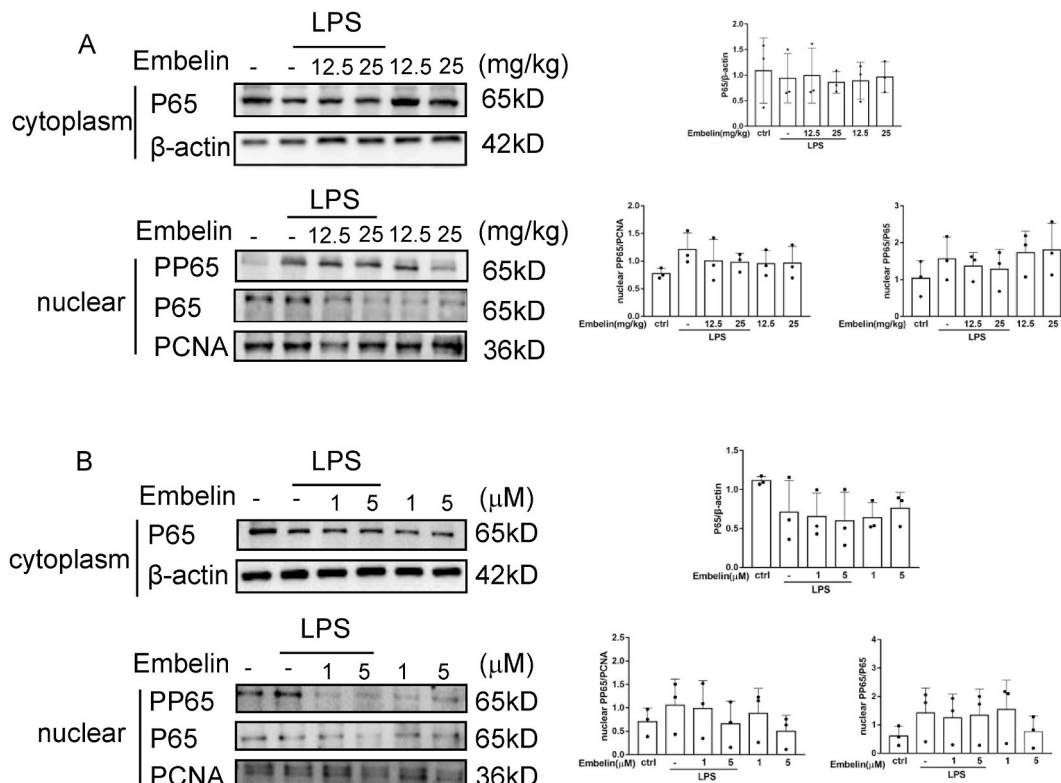


**Fig. 11. Embelin represses the expression of phosphorylated NF- $\kappa$ B p65 through the ser536 site *in vivo* and *in vitro*.** After total protein detected by WB, plasma proteins were used for the detection of p65. Additionally, nuclear proteins were isolated for further detection of p65 and pp65, and PCNA was used as the loading control in the nuclear fraction. All bands were quantitatively analyzed using ImageJ software and are shown on the right. A) The expression of phosphorylated NF- $\kappa$ B p65 at ser536 in the nucleus *in vivo*. B) The expression of phosphorylated NF- $\kappa$ B p65 at ser536 in the nucleus *in vitro*. Images shown are representative of three independent experiments, and data are presented as the mean  $\pm$  standard deviation (SD).

To elucidate the therapeutic mechanisms of embelin on AKI, we performed bioinformatic analysis. We identified some inflammatory pathways associated with both AKI and embelin, including the NF- $\kappa$ B, TNF, Jak-STAT, and toll-like receptor signaling pathways. During sepsis, LPS could activate the TLR4 inflammatory signal pathway by directly binding to the pattern recognition receptors of immune cells, thereby releasing inflammatory cytokines to damage the tissues and organs [40]. The NF- $\kappa$ B signaling pathway is key to the immunomodulation of inflammation by TLR4 signaling [41–43]. Under inflammatory conditions, the expression of p-I $\kappa$ B $\alpha$ , p-p65, and TLR4 significantly increases [44,45]. In our study, embelin suppressed the expression of TLR4 and the phosphorylation of I $\kappa$ B $\alpha$  and NF- $\kappa$ B p65 in murine kidneys following LPS injection. Notably, LPS can promote the expression of TLR4, p-I $\kappa$ B $\alpha$ , and p-p65 when macrophages are activated [46–48]. We observed that embelin could inhibit the expression of TLR4 and the phosphorylation of I $\kappa$ B $\alpha$  and NF- $\kappa$ B p65 in murine BMDMs following LPS stimulation. Embelin also inhibited the secretion of IL-1 $\beta$  and IL-6 and increased the secretion of Arg-1 and IL-10 in both LPS- and NF- $\kappa$ B activator BA-treated murine BMDMs. The results showed that embelin inhibited the expression of TLR4 and the phosphorylation of I $\kappa$ B $\alpha$  and NF- $\kappa$ B p65 both *in vivo* and *in vitro*.

When LPS induces macrophage activation, NF- $\kappa$ B signaling is activated, and phosphorylated NF- $\kappa$ B p65 can be translocated. NF- $\kappa$ B p65 in the cytoplasm is phosphorylated and translocated to the nucleus, and the level of phosphorylated NF- $\kappa$ B p65 in the nucleus is significantly increased [22]. We observed a reduction in NF- $\kappa$ B p65 levels in the cytoplasm of murine renal tissues and murine BMDMs after embelin treatment and LPS stimulation. The results of molecular docking predicted that embelin could bind to phosphorylated NF- $\kappa$ B p65 at the ser536 site. We also observed that embelin could significantly reduce the levels of total NF- $\kappa$ B p65 and NF- $\kappa$ B p65 phosphorylated at ser536 in the nuclei of murine renal tissues and murine BMDMs following LPS stimulation. These findings suggest that embelin inhibits phosphorylation at the ser536 site and the translocation of NF- $\kappa$ B p65 from the cytosol to the nucleus.

Embelin also caused an increase in the secretion of Arg-1 and IL-10 in the supernatants of BMDMs following LPS stimulation, as well as the expression of CD206 in the kidney of mice treated with LPS. These results indicate the potential role of embelin in M2 macrophage turnover, suggesting a limitation to the current study; we did not elucidate the effects and mechanisms of embelin in M2 macrophage polarization. Our future studies will focus on unveiling the potential role of embelin in M2 macrophages in septic AKI.

Another limitation of the current study is that several recent studies on the potential of natural products for treating septic AKI have been performed. Although they show a wide range of clinical prospects for treating septic AKI, most of these natural products are still in the preclinical research stage owing to problems with low solubility, low bioavailability, and inappropriate dosage. The current study

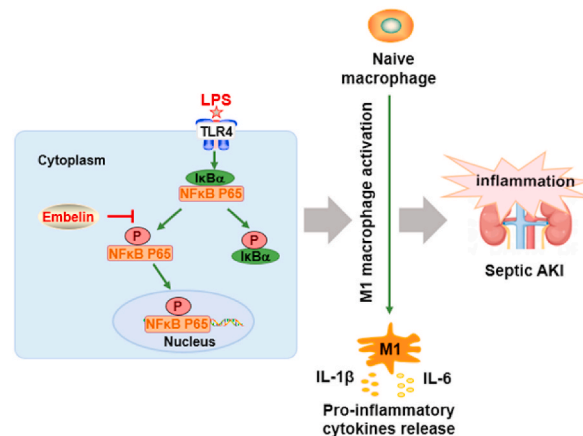


**Fig. 12.** Schematic diagram summarizing the mechanism of action of embelin in LPS-induced AKI via the NF- $\kappa$ B signaling pathway.

only included the clinical drug DEX and the new candidate natural drug ISL as the positive controls to identify the suppressive role of embelin in septic AKI via the immunomodulation of macrophages. Therefore, we aim to optimize the preparation of embelin to solve the problems of low solubility, low bioavailability, and inappropriate dosage in septic AKI treatment.

In conclusion, we evaluated the immunomodulatory and anti-inflammatory effects of embelin on murine AKI caused by LPS and demonstrated that embelin could attenuate LPS-induced AKI by impairing M1 macrophage activation and NF- $\kappa$ B signaling in mice (Fig. 12). The study findings preclinically suggest a potential therapeutic role of embelin in septic AKI.

#### Author contribution statement

Qiao Tang: Conceived and designed the experiments; Performed the experiments; Analyzed and interpreted the data; Wrote the paper.

Yun Tang; Qun Yang; Rong Chen; Hong Zhang; Liming Huang; Jie Chen; Lin Wang: Performed the experiments.

Haojun Luo; Qiong Xiao; Kaixiang Liu; Xinrou Song; Sipei Chen: Contributed reagents, materials, analysis tools or data.

Guisen Li; Li Wang: Analyzed and interpreted the data.

YI LI: Conceived and designed the experiments; Analyzed and interpreted the data; Wrote the paper.

#### Funding statement

Li Wang was supported by National Natural Science Foundation of China [U21A20349; 8170742], Key Research and Development Program of Sichuan Province [2021YFS0370].

Dr. YI LI was supported by National Natural Science Foundation of China [82270729 and 81700607].

Guisen Li was supported by Key Research and Development Program of Sichuan Province [2019YFS0538], National Natural Science Foundation of China [82070690].

#### Data availability statement

Data will be made available on request.

#### Declaration of interest's statement

The authors declare no competing interests.

#### Acknowledgments

The authors are grateful to Prof. Zhenglin Yang and Prof. Shaoping Deng of the University of Electronic Science and Technology, Sichuan Academy of Medical Sciences & Sichuan Provincial People's Hospital, for generously providing research platforms and technical support. The authors would also like to thank Xu Xiang from the Clinical Immunology Translational Medicine Key Laboratory of Sichuan Province, School of Medicine, University of Electronic Science, and Technology of China.

#### Appendix A. Supplementary data

Supplementary data to this article can be found online at <https://doi.org/10.1016/j.heliyon.2023.e14006>.

## References

- [1] M. Singer, C.S. Deutschman, C.W. Seymour, M. Shankar-Hari, D. Annane, M. Bauer, R. Bellomo, G.R. Bernard, J.D. Chiche, C.M. Coopersmith, R.S. Hotchkiss, M. M. Levy, J.C. Marshall, G.S. Martin, S.M. Opal, G.D. Rubenfeld, T. van der Poll, J.L. Vincent, D.C. Angus, The third international consensus definitions for sepsis and septic shock (Sepsis-3), *JAMA* 315 (8) (2016) 801–810.
- [2] S. Uchino, J.A. Kellum, R. Bellomo, G.S. Doig, H. Morimatsu, S. Morgera, M. Schetz, I. Tan, C. Bouman, E. Macedo, N. Gibney, A. Tolwani, C. Ronco, Acute renal failure in critically ill patients: a multinational, multicenter study, *JAMA* 294 (7) (2005) 813–818.
- [3] S.M. Bagshaw, S. Lapinsky, S. Dial, Y. Arabi, P. Dodek, G. Wood, P. Ellis, J. Guzman, J. Marshall, J.E. Parrillo, Y. Skrobik, A. Kumar, Acute kidney injury in septic shock: clinical outcomes and impact of duration of hypotension prior to initiation of antimicrobial therapy, *Intensive Care Med.* 35 (5) (2009) 871–881.
- [4] G.M. Gonçalves, D.S. Zamboni, N.O. Câmara, The role of innate immunity in septic acute kidney injuries, *Shock* 34 (Suppl 1) (2010) 22–26.
- [5] H.G. Kang, H.K. Lee, K.B. Cho, S.I. Park, A review of natural products for prevention of acute kidney injury, *Medicina* 57 (11) (2021).
- [6] Y.L. Feng, Y. Yang, H. Chen, Small molecules as a source for acute kidney injury therapy, *Pharmacol. Ther.* 237 (2022), 108169.
- [7] H. Fan, B.J. Su, J.W. Le, J.H. Zhu, Salidroside protects acute kidney injury in septic rats by inhibiting inflammation and apoptosis, *Drug Des. Dev. Ther.* 16 (2022) 899–907.
- [8] Y. Tang, H. Luo, Q. Xiao, L. Li, X. Zhong, J. Zhang, F. Wang, G. Li, L. Wang, Y. Li, Isoliquiritigenin attenuates septic acute kidney injury by regulating ferritinophagy-mediated ferroptosis, *Ren. Fail.* 43 (1) (2021) 1551–1560.
- [9] L. Chen, Y. Lu, L. Zhao, L. Hu, Q. Qiu, Z. Zhang, M. Li, G. Hong, B. Wu, G. Zhao, Z. Lu, Curcumin attenuates sepsis-induced acute organ dysfunction by preventing inflammation and enhancing the suppressive function of Tregs, *Int. Immunopharm.* 61 (2018) 1–7.
- [10] H. Li, H. Sun, Y. Xu, G. Xing, X. Wang, Curcumin plays a protective role against septic acute kidney injury by regulating the TLR9 signaling pathway, *Transl. Androl. Urol.* 10 (5) (2021) 2103–2112.
- [11] Y. Cai, C. Huang, M. Zhou, S. Xu, Y. Xie, S. Gao, Y. Yang, Z. Deng, L. Zhang, J. Shu, T. Yan, C.C. Wan, Role of curcumin in the treatment of acute kidney injury: research challenges and opportunities, *Phytomedicine* 104 (2022), 154306.
- [12] N.Z. Ning, X. Liu, F. Chen, P. Zhou, L. Hu, J. Huang, Z. Li, J. Huang, T. Li, H. Wang, Embelin restores carbapenem efficacy against NDM-1-positive pathogens, *Front. Microbiol.* 9 (2018) 71.
- [13] J.L. Allensworth, K.M. Aird, A.J. Aldrich, I. Batinic-Haberle, G.R. Devi, XIAP inhibition and generation of reactive oxygen species enhances TRAIL sensitivity in inflammatory breast cancer cells, *Mol. Cancer Therapeut.* 11 (7) (2012) 1518–1527.
- [14] S. Durg, V.P. Veerapur, S. Neelima, S.B. Dhadde, Antidiabetic activity of *Embelia ribes*, embelin and its derivatives: a systematic review and meta-analysis, *Biomed. Pharm.* 86 (2017) 195–204.
- [15] R. Poojari, Embelin - a drug of antiquity: shifting the paradigm towards modern medicine, *Exp. Opin. Invest. Drugs* 23 (3) (2014) 427–444.
- [16] K.S. Ahn, G. Sethi, B.B. Aggarwal, Embelin, an inhibitor of X chromosome-linked inhibitor-of-apoptosis protein, blocks nuclear factor-kappaB (NF-kappaB) signaling pathway leading to suppression of NF-kappaB-regulated antiapoptotic and metastatic gene products, *Mol. Pharmacol.* 71 (1) (2007) 209–219.
- [17] H. Wang, H. Zhang, Y. Wang, L. Yang, D. Wang, Embelin can protect mice from thioacetamide-induced acute liver injury, *Biomed. Pharm.* 118 (2019), 109360.
- [18] S. Azman, M. Sekar, S. Wahidin, S.H. Gan, J. Vajjanathappa, S.R. Bonam, M. Alvata, P.T. Lum, V. Thakur, J.V. Beladiya, A.A. Mehta, Embelin alleviates severe airway inflammation in OVA-LPS-induced rat model of allergic asthma, *J. Asthma Allergy* 14 (2021) 1511–1525.
- [19] S. Gordon, F.O. Martinez, Alternative activation of macrophages: mechanism and functions, *Immunity* 32 (2010) 593–604.
- [20] J.A. Reynolds, E.M. McCarthy, S. Haque, P. Ngamjanyaporn, J.C. Sergeant, E. Lee, E. Lee, S.A. Kilfeather, B. Parker, I.N. Bruce, Cytokine profiling in active and quiescent SLE reveals distinct patient subpopulations, *Arthritis Res. Ther.* 20 (1) (2018) 173.
- [21] J. Zhang, Y. Zhang, F. Xiao, Y. Liu, J. Wang, H. Gao, S. Rong, Y. Yao, J. Li, G. Xu, The peroxisome proliferator-activated receptor  $\gamma$  agonist pioglitazone prevents NF- $\kappa$ B activation in cisplatin nephrotoxicity through the reduction of p65 acetylation via the AMPK-SIRT1/p300 pathway, *Biochem. Pharmacol.* 101 (2016) 100–111.
- [22] Y. Tang, C. Wang, S. Chen, L. Li, X. Zhong, J. Zhang, Y. Feng, L. Wang, J. Chen, M. Yu, F. Wang, L. Wang, G. Li, Y. He, Y. Li, Dimethyl fumarate attenuates LPS induced septic acute kidney injury by suppression of NF $\kappa$ B p65 phosphorylation and macrophage activation, *Int. Immunopharm.* 102 (2022), 108395.
- [23] C.J. Watson, N. Glezeva, S. Horgan, J. Gallagher, D. Phelan, K. McDonald, M. Tolan, J. Baugh, P. Collier, M. Ledwidge, Atrial tissue pro-fibrotic M2 macrophage marker CD163+, gene expression of procollagen and B-type natriuretic peptide, *J. Am. Heart Assoc.* 9 (11) (2020), e013416.
- [24] X. Zhao, J. Qu, X. Liu, J. Wang, X. Ma, X. Zhao, Q. Yang, W. Yan, Z. Zhao, Y. Hui, H. Bai, S. Zhang, Baicalein suppress EMT of breast cancer by mediating tumor-associated macrophages polarization, *Am. J. Canc. Res/* 8 (8) (2018) 1528–1540.
- [25] D.B. Kitchen, H. Decornez, J.R. Furr, J. Bajorath, Docking and scoring in virtual screening for drug discovery: methods and applications, *Nat. Rev. Drug Discov.* 3 (11) (2004) 935–949.
- [26] A.M. Schaible, H. Traber, V. Temml, S.M. Noha, R. Filosa, A. Peduto, C. Weinigel, D. Barz, D. Schuster, O. Werz, Potent inhibition of human 5-lipoxygenase and microsomal prostaglandin  $E_2$  synthase-1 by the anti-carcinogenic and anti-inflammatory agent embelin, *Biochem. Pharmacol.* 86 (2013) 476–486.
- [27] S.R. Naik, N.T. Nitire, A.A. Ansari, P.D. Shah, Anti-diabetic activity of embelin: involvement of cellular inflammatory mediators, oxidative stress and other biomarkers, *Phytomedicine* 20 (2013) 797–804.
- [28] S. Watanabe, M. Alexander, A.V. Misharin, G.R.S. Budinger, The role of macrophages in the resolution of inflammation, *J. Clin. Invest.* 129 (2019) 2619–2628.
- [29] X.Q. Liu, J. Jin, Z. Li, L. Jiang, Y.H. Dong, Y.T. Cai, M.F. Wu, J.N. Wang, T.T. Ma, J.G. Wen, M.M. Liu, J. Li, Y.G. Wu, X.M. Meng, Rutaecarpine derivative Cpd-6c alleviates acute kidney injury by targeting PDE4B, a key enzyme mediating inflammation in cisplatin nephropathy, *Biochem. Pharmacol.* 180 (2020) 114132–114176.
- [30] X. Qin, L. Hu, S.N. Shi, X. Chen, C. Zhuang, W. Zhang, S. Jitkaew, X. Pang, J. Yu, Y.X. Tan, H.Y. Wang, Z. Cai, The bcr-abl inhibitor GNF-7 inhibits necroptosis and ameliorates acute kidney injury by targeting RIPK1 and RIPK3 kinases, *Biochem. Pharmacol.* 177 (2020), 113947.
- [31] X.X. Yan, A.D. Zheng, Z.E. Zhang, G.C. Pan, W. Zhou, Protective effect of pantoprazole against sepsis-induced acute lung and kidney injury in rats, *Am. J. Transl. Res.* 11 (2019) 5197–5211.
- [32] Y. Li, P. Zhai, Y. Zheng, J. Zhang, J.A. Kellum, Z. Peng, Csf2 attenuated sepsis-induced acute kidney injury by promoting alternative macrophage transition, *Front. Immunol.* 11 (2020) 1415.
- [33] R.W. Hallowell, S.L. Collins, J.M. Craig, Y. Zhang, M. Oh, P.B. Illei, Y. Chan-Li, C.L. Vigeland, W. Mitzner, A.L. Scott, J.D. Powell, M.R. Horton, mTORC2 signalling regulates M2 macrophage differentiation in response to helminth infection and adaptive thermogenesis, *Nat. Commun.* 8 (2017), 14208.
- [34] F. Wang, S. Zhang, R. Jeon, I. Vuckovic, X. Jiang, A. Lerman, C.D. Folmes, P.D. Dzeja, J. Herrmann, Interferon gamma induces reversible metabolic reprogramming of M1 macrophages to sustain cell viability and pro-inflammatory activity, *EBioMedicine* 30 (2018) 303–316.
- [35] S. Palaniyandi, R. Kumari, S. Venniyil Radhakrishnan, E. Stratton, N. Hakim, R. Munker, M.V. Kesler, G.C. Hildebrandt, The prolyl hydroxylase inhibitor dimethyl oxalyl glycine decreases early gastrointestinal GVHD in experimental allogeneic hematopoietic cell transplantation, *Transplantation* 104 (2020) 2507–2515.
- [36] D.Y. Vogel, P.D. Heijnen, M. Breur, H.E. de Vries, A.T. Tool, S. Amor, C.D. Dijkstra, Macrophages migrate in an activation-dependent manner to chemokines involved in neuroinflammation, *J. Neuroinflammation* 11 (2014) 23.
- [37] L. Qin, X. Wu, M.L. Block, Y. Liu, G.R. Breese, J.S. Hong, D.J. Knapp, F.T. Crews, Systemic LPS causes chronic neuroinflammation and progressive neurodegeneration, *Glia* 55 (2007) 453–462.
- [38] A. Torres-Espín, J. Forero, K.K. Fenrich, A.M. Lucas-Osma, A. Krajacic, E. Schmidt, R. Vavrek, P. Raposo, D.J. Bennett, P.G. Popovich, K. Fouad, Eliciting inflammation enables successful rehabilitative training in chronic spinal cord injury, *Brain* 141 (2018) 1946–1962.
- [39] Z. Nikolovska-Coleska, L. Xu, Z. Hu, Y. Tomita, P. Li, P.P. Roller, R. Wang, X. Fang, R. Guo, M. Zhang, M.E. Lippman, D. Yang, S. Wang, Discovery of embelin as a cell-permeable, small-molecular weight inhibitor of XIAP through structure-based computational screening of a traditional herbal medicine three-dimensional structure database, *J. Med. Chem.* 47 (2004) 2430–2440.

- [40] G. Maiti, J. Frikeche, C.Y. Lam, A. Biswas, V. Shinde, M. Samanovic, J.C. Kagan, M.J. Mulligan, S. Chakravarti, Matrix lumican endocytosed by immune cells controls receptor ligand trafficking to promote TLR4 and restrict TLR9 in sepsis, *Proc. Natl. Acad. Sci. U. S. A* 118 (27) (2021).
- [41] T. Lawrence, The nuclear factor NF-kappaB pathway in inflammation, *Cold Spring Harbor Perspect. Biol.* 1 (2009) a001651.
- [42] B. Hoesel, J.A. Schmid, The complexity of NF- $\kappa$ B signaling in inflammation and cancer, *Mol. Cancer* 12 (2013) 86.
- [43] M.S. Schappe, K. Sztejn, M.E. Stremaska, S.K. Mendu, T.K. Downs, P.V. Seegren, M.A. Mahoney, S. Dixit, J.K. Krupa, E.J. Stipes, J.S. Rogers, S.E. Adamson, N. Leitinger, B.N. Desai, Chanzyme TRPM7 mediates the Ca(2+) influx essential for lipopolysaccharide-induced toll-like receptor 4 endocytosis and macrophage activation, *Immunity* 48 (1) (2018) 59–74.e5.
- [44] F. Dai, Y.T. Du, Y.L. Zheng, B. Zhou, Inhibiting NF- $\kappa$ B-mediated inflammation by catechol-type diphenylbutadiene via an intracellular copper- and iron-dependent pro-oxidative role, *J. Agric. Food Chem.* 68 (2020) 10029–10035.
- [45] H. Lu, L. Wu, L. Liu, Q. Ruan, X. Zhang, W. Hong, S. Wu, G. Jin, Y. Bai, Quercetin ameliorates kidney injury and fibrosis by modulating M1/M2 macrophage polarization, *Biochem. Pharmacol.* 154 (2018) 203–212.
- [46] R. Chen, L. Zeng, S. Zhu, J. Liu, H.J. Zeh, G. Kroemer, H. Wang, T.R. Billiar, J. Jiang, D. Tang, R. Kang, cAMP metabolism controls caspase-11 inflammasome activation and pyroptosis in sepsis, *Sci. Adv.* 5 (2019) eaav5562.
- [47] M. Liu, L. Yin, W. Li, J. Hu, H. Wang, B. Ye, Y. Tang, C. Huang, C1q/TNF-related protein-9 promotes macrophage polarization and improves cardiac dysfunction after myocardial infarction, *J. Cell. Physiol.* 234 (2019) 18731–18747.
- [48] H. Gao, Y. Cui, N. Kang, X. Liu, Y. Liu, Y. Zou, Z. Zhang, X. Li, S. Yang, J. Li, C. Wang, Q.M. Xu, X. Chen, Isoacteoside, a dihydroxyphenylethyl glycoside, exhibits anti-inflammatory effects through blocking toll-like receptor 4 dimerization, *Br. J. Pharmacol.* 174 (2017) 2880–2896.